Influence of self-affine roughness on Parsons-Zobel plots for electrical double layers

G. Palasantzas*
Department of Applied Physics and Materials Science Centre, University of Groningen, Nijenborgh 4, 9747 AG Groningen, The Netherlands

G. M. E. A. Backx
Computational Physics Centre, Briljantstraat 341, 9743 NM Groningen, The Netherlands
(Received 15 December 2003; published 30 April 2004)

In this paper we investigate the dependence of Parsons-Zobel plots on characteristic self-affine roughness parameters of the metal electrode in electrical double layers. Among the roughness amplitude w, the correlation length ξ, and roughness exponent H, the latter appears to have the most prominent effect especially for values in the range $H<0.5$. In addition, with decreasing compact layer thickness the influence of roughness leads to stronger nonlinear behavior of the plots for relatively large electrode potentials. Finally, it is shown that dynamic changes of the electrode roughness (for example by growth on metal films) should be carefully quantified with respect to their influence on the Parson-Zobel plots and related double-layer systems.

DOI: 10.1103/PhysRevE.69.041603 PACS number(s): 68.08.−p, 73.61.−r, 41.20.Cv, 68.55.−a

I. INTRODUCTION

Many important applications in electrochemistry [1], colloid science [2], biophysics [3], semiconductor microelectronics [4], etc., are based on the Gouy-Chapman (GC) [5,6] theory of electrolyte plasma near a flat charged electrode. Although, for a long period electrochemical studies were performed with a liquid mercury drop electrode (and later with GaTi, Ga, InGa, etc., electrodes) [7], studies with solid electrodes (Cd, Bi, Cu, Pb) indicated that the metal/electrolyte interface roughness has to be taken very carefully into account [8]. Indeed, for flat metal/electrolyte interfaces, the GC theory yields a space charge capacitance [5,6] $C_{\mathrm{GC}}=(\varepsilon S_{flat}/4\pi\lambda_{\mathrm{D}})\cosh(e\beta\Phi_{\mathrm{o}})$ with ε the solvent dielectric constant, $\beta=1/K_BT$ with K_B the Boltzmann constant and T the system temperature, e the electron charge, Φ_{o} the electrode potential, S_{flat} the flat electrolyte/metal electrode interface area, and λ_{D} the Debye length [6]. The latter measures the separation of charge and counter charge in the electrolyte plasma.

However, for rough interfaces, S_{flat} cannot be simply replaced by RS_{flat}, where R is the geometric ratio of the true surface to the apparent flat cross-section area S_{flat}. This is because characteristic lateral roughness length scales can compete with system characteristic length scales (i.e., the Debye length λ_{D}) leading to different functional dependence on potential and electrolyte concentration [9]. The theory by Daikhin *et al.* [9] was applied for electric double layers with Bi, Sb, and Cd electrodes [10]. Deviations between experimental and theoretical roughness function versus inverse Debye length curves were explained by the influence of energetic inhomogeneity of polycrystalline surfaces on the nonequal surface charge density at various homogeneous regions exposed at the macropolycrystalline electrode surfaces [10]. Furthermore, extension of the theory to the case of the nonlinear Poisson-Boltzmann (PB) theory was performed by Daikhin *et al.* [11] and Lust *et al.* [12] who explained successfully data for Cd rough electrodes.

So far in the original work by Daikhin *et al.* [11] within the nonlinear regime of the Poisson-Boltzmann theory, the case of weak roughness was explored (sinusoidal corrugation and Gaussian roughness). In this work, various investigations were also made for Parsons-Zobel (PZ) plots. The PZ plots are plots of inverse total capacitance (diffuse and compact layer) versus the inverse GC capacitance. These plots are used to test the validity of the GC theory, where a straight line with unit slope approves the GC theory for the diffuse layer with the corresponding intercept yielding the inverse capacitance of the compact layer [11]. Slopes lower than one are usually related to the geometrical roughness factor R [13], while any deviations from linear behavior are considered as indications of specific adsorption of ions, incomplete dissociation of electrolyte [8], crystallographic inhomogeneity [8,13–16], and electrode roughness within the nonlinear PB theory [11].

In this work, we will investigate the sensitivity of PZ plots on the characteristic parameters of self-affine rough surfaces. Computation of the PZ plots will be performed within the nonlinear PB theory for weak electrode roughness [9,11,13]. In the latter case, analytic calculations of the local interface slope will further facilitate results for double-layer properties. Finally, the sensitivity of PZ plots on changes of the metal electrode roughness by growth process will also be investigated.

II. BRIEF DOUBLE-LAYER THEORY

We assume that the rough metal/electrolyte interface (held at potential Φ_{o}) can be described by a single-valued random function $z=h(R_{in})$ of the in-plane position vector $R_{in}=(x,y)$

*Corresponding author.
Email address: G.Palasantzas@phys.rug.nl

with the average flat interface area at $z=0$ [$\langle h(R_{in})\rangle=0$]. For any electrostatic potential $\Phi(r)$, one has to solve the nonlinear Poisson-Boltzmann equation $\nabla^2\Phi-(k_D{}^2/e\beta)\sinh(e\beta\Phi)=0$ ($k_D=1/\lambda_D$) with boundary conditions $\Phi(x,y,z=h(x,y))=\Phi_o$ and $\Phi(x,y,z\to+\infty)=0$ assuming that the electrolyte occupies the half space $z>0$ [11]. In the weak roughness limit ($|\nabla h|\ll 1$ and $h\ll\lambda_D$), the diffuse capacitance C is given by [11]

$$C=\tilde{R}C_{GC},\quad \tilde{R}=1+\frac{1}{2}\int_{0<q<Q_c}F(q)\langle|h(q)|^2\rangle\frac{d^2q}{(2\pi)^2} \quad (1)$$

with $F(q)=q^2\{1-q^2[M(q)-K_{eff}+2(\lambda_D^{-2}/K_{eff})][K_{eff}+M(q)]^{-3}\}$, and ε the dielectric constant of the electrolyte solvent. Moreover, we have $M(q)=\sqrt{\lambda_D^{-2}+q^2}$, $K_{eff}=\lambda_D^{-1}\cosh(e\beta\Phi_o)$, and $C_{GC}=(\varepsilon/4\pi)K_{eff}$ [11]. In Eq. (1) the term $\langle|h(q)|^2\rangle$ is the metal/electrolyte interface roughness spectrum. Furthermore, the requirement of weak roughness for the validity of Eqs. (1) can be reformulated more precisely. Indeed, we require the average interface slope to be small or $\rho_{rms}=\sqrt{\langle|\nabla h|^2\rangle}\ll 1$, and $w/\lambda_D\ll 1$ with $w=\sqrt{\langle h^2\rangle}$ the rms roughness amplitude. Notably, the local slope ρ_{rms} is given in terms of the roughness spectrum $\langle|h(q)|^2\rangle$ by

$$\rho_{rms}=\left\{\int_{0<q<Q_c}q^2\langle|h(q)|^2\rangle\frac{d^2q}{(2\pi)^2}\right\}^{1/2} \quad (2)$$

with $Q_c=\pi/c$ and c a lower length scale cutoff of the order of atomic dimensions.

The total capacitance C_T is obtained by the diffuse capacitance C and the compact layer capacitance C_H assuming a series connection [11,17],

$$\frac{1}{C_T}=\frac{1}{C}+\frac{1}{C_H}. \quad (3)$$

The capacitance C_H is due to a thin layer (of several angstrom thickness L_H) of solvent molecules at the metal/solvent interface with dielectric constant ε_* different than that of the bulk electrolyte where the GC theory is applicable [11,17]. For a flat interface we have $C_{H,flat}=\varepsilon_*/4\pi L_H$ [17], while for a rough one [11]

$$C_H=RC_{H,flat},\quad R=\int_0^{+\infty}(1+\rho_{rms}{}^2u)^{1/2}e^{-u}du \quad (4)$$

under the restrictions that the layer thickness is smaller than all characteristic roughness length scales ($L_H<w,\xi$). For the calculation of the area ratio R we have assumed a Gaussian height-height distribution [18,19]. Finally, we should point out that Eq. (3) is based on the assumption that the compact layer/diffuse interface is equipotential. The assumption of equipotential interface may be cast into doubt for rough metal electrode surfaces, since different crystal faces can be exposed with different dipole potential drop across the corresponding segments of the compact layer [8,11]. However, since the crystalline heterogeneity on flat surfaces for many metals [8] has not shown drastic effect, we will still assume the validity of Eq. (3).

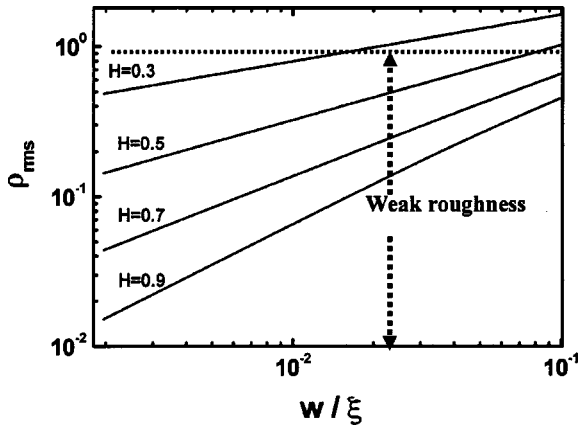

FIG. 1. Local surfaces slope vs th roughness ratio w/ξ for various roughness exponents H, with the dotted line indicating the regime of $\rho_{rms}<1$.

III. RESULTS AND DISCUSSION

In the following we will consider a model for the roughness spectrum $\langle|h(q)|^2\rangle$ which is necessary for the calculation of the capacitance terms in Eq. (3). A wide variety of surfaces and interfaces appearing in various physical systems (i.e., films grown under nonequilibrium conditions) possess roughness, which is termed as self-affine [20]. The latter is characterized by a finite correlation length ξ, a rms roughness amplitude w, and a roughness exponent $H(0<H<1)$. This is a measure of the degree of surface irregularity [20,21] so that small values of $H(\sim 0)$ characterize extremely jagged or irregular surfaces, while large values of $H(\sim 1)$ surfaces with smooth hills and valleys [20]. For self-affine roughness, the spectrum $\langle|h(q)|^2\rangle$ has a power law scaling behavior: $\langle|h(q)|^2\rangle\propto q^{-2-2H}$ if $q\xi\gg 1$ and $\langle|h(q)|^2\rangle\propto$ const if $q\xi\ll 1$ [20]. This scaling behavior is satisfied by the simple Lorentzian model [21]

$$\langle|h(q)^2|\rangle=\frac{2\pi w^2\xi^2}{(1+aq^2\xi^2)^{1+H}}, \quad (5)$$

where $a=(1/2H)[1-(1+aQc^2\xi^2)^{-H}]$, and $Q_c=\pi/c$ with c a lower roughness cutoff of the order of atomic dimensions.

The inverse total capacitance is given by Eqs. (1), (3), and (4) in the form

$$\frac{1}{C_T}=\frac{1}{C_{GC}}\left[\frac{1}{\tilde{R}}+\frac{1}{R}\frac{\varepsilon}{\varepsilon_*}\frac{L_H}{\lambda_D}\cosh(e\beta\Phi_o)\right]. \quad (6)$$

For simplicity we performed calculations of C_T in terms of Eq. (6) by setting $\varepsilon_*=\varepsilon$. Moreover, we considered the effective potential $e\beta\Phi_o<20$ range, which is well within the nonlinear regime of the PB theory. Similar plots can be performed for various electrolyte concentrations "n" since $\lambda_D=(\varepsilon\beta/8\pi e^2n)^{1/2}$. Moreover, the calculations of C_T were performed for small local interface slopes so that $\rho_{rms}=\sqrt{\langle|\nabla h|^2\rangle}<1$ (see Fig. 1) [22]. Although for the lower

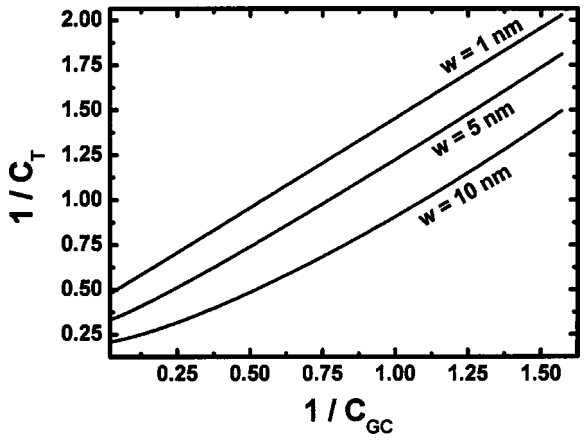

FIG. 2. PZ plot for various values of the roughness amplitude w for $H=0.5$, $\xi=200$ nm, $L_H=3$ nm, and $\lambda_D=10$ nm.

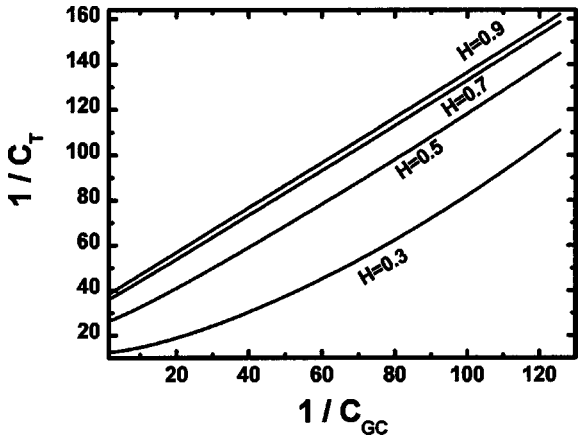

FIG. 4. PZ plot for various values of the roughness exponent H for $\xi=200$ nm, $w=5$ nm, $L_H=3$ nm, and $\lambda_D=10$ nm.

roughness cutoff we have considered the value $c=0.3$ nm (typical lattice constant of metals), a lower value might be necessary for a particular system (depending on the material) because the actual smallest step height might be smaller than the lattice constant.

Figure 2 shows the PZ plots for various roughness amplitudes w. When the latter is relatively small so that $\rho_{rms}<1$, the PZ plot appears rather linear. Any deviation from the linear behavior is characteristic for the presence of increased surface roughness for large GC-capacitance values or alternatively elevated effective electrode potentials $e\beta\Phi_0>1$ (typical for the nonlinear regime). Although $\langle|h(q)^2|\rangle\sim w^2$ which implies directly that $\tilde{R}\sim w^2$ and thus for the diffuse capacitance the dependence $1/C\sim w^{-2}$, the geometrical roughness term R yields a nonlinear dependence on the rms roughness amplitude w and thus for the PZ plots. Indeed, Eq. (5) yields $\rho_{rms}=(w/\sqrt{2}a\xi)\{(1-H)^{-1}[(1+aQ_c{}^2\xi)^{1-H}-1]-2a\}^{1/2}$ [22], which follows the scaling behavior $\rho_{rms}\sim w/\xi^H$ after simplifications for $Q_c\xi\gg1$ and $0<H<1$.

Similar to the influence of the roughness amplitude w, it is also the influence of decreasing lateral correlation ξ (Fig. 3) or increasing long wavelength electrode roughness. In this case, the nonlinear behavior at high GC-capacitance values comes from both the geometrical roughness factor R and the factor $\tilde{R}$ that is related to the diffuse capacitance C [as Eq. (1) indicates]. This is because the dependence of both terms on the correlation length ξ is more complex than that of the roughness amplitude w. In addition, the PZ plots show a significant sensitivity and deviations from linear behavior at large GC-capacitance values for decreasing roughness exponent H (<0.5) as Fig. 4 indicates. If we compare Figs. 2–4, it is clear that the short wavelength roughening, as expressed by lower values of the roughness exponent H, appears to have the dominant effect on the PZ plots. This is also expected from the fact that the local slope $\rho_{rms}(\sim w/\xi^H)$ is dominated by the contribution of the exponent H rather than the long wavelength ratio w/ξ as also Fig. 1 indicates.

We should point out that for sufficiently rough metal surfaces ($H\ll1$ and $w/\xi\sim1$ yielding strong roughness or $\rho_{rms}\gg1$) the diffuse layer/compact layer interface will not have the same roughness parameters even for thin compact layers. However, for weak roughness ($\rho_{rms}<1$), which is under consideration in this work, we can omit this complication. At any rate, the PZ plot is also shown to be sensitive to changes of the compact layer thickness L_H (Fig. 5) within the nonlinear regime or for large GC-capacitance values, with an increasing nonlinear behavior for layer compact thicknesses $L_H<1$ nm.

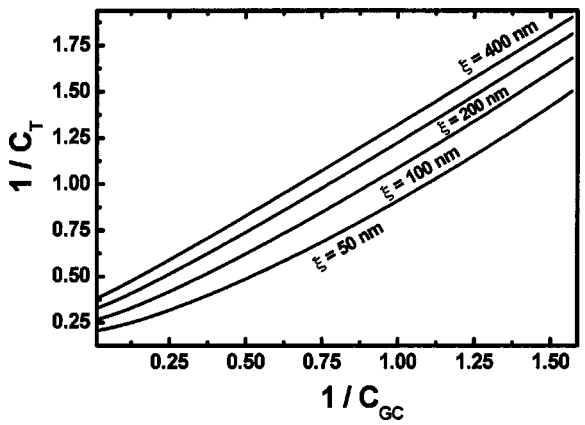

FIG. 3. PZ plot for various values of the lateral correlation length ξ for $w=5$ nm, $H=0.5$, $L_H=3$ nm, and $\lambda_D=10$ nm.

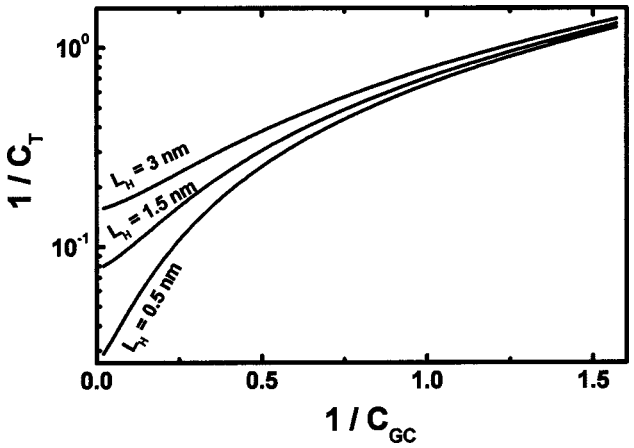

FIG. 5. PZ plot for various values of the compact layer thickness L_H for $H=0.3$, $\xi=200$ nm, $w=5$ nm, and $\lambda_D=10$ nm.

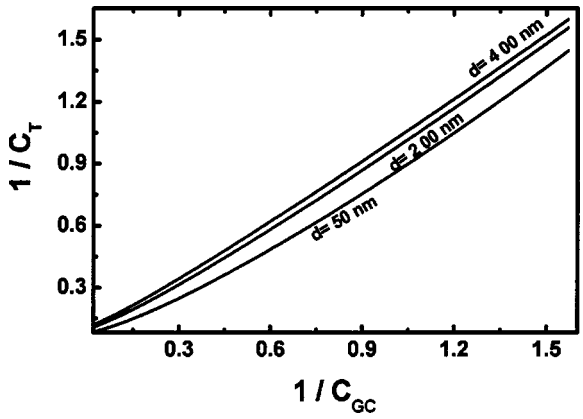

FIG. 6. PZ plot for various values of the metal thickness d for the metal electrode $L_H=1$ nm, and $\lambda_D=10$ nm. The plots were performed with $w=5(d/100)^{0.25}$ and $\xi=100(d/100)^{2(0.25/H)}$ for $H=0.5$.

Finally, we will investigate the possibility of the variation of the metal electrode roughness by depositing metal, for example of thickness d, and its influence on the PZ plots. For normal self-affine growth, which occurs for constant roughness exponents H (independent of film thickness) and obeys the dynamic scaling hypothesis (with w and ξ growing as power laws $w \propto d^{\beta}$ and $\xi \propto d^{\beta/H}$ where β is the growth exponent), the local slope (which scales as $\rho_{rms} \sim w/\xi^{H}$) remains a time or thickness invariant of the growing front (assuming constant deposition rate) [20]. As a result, the PZ plots remain unaffected by this type of electrode roughness variation, which is also in agreement with direct calculations.

If, however, we assume that the correlation length evolves, i.e., with a different power law say $\xi \propto d^{2\beta/H}$ yielding thus an evolving local slope $\rho_{rms} \sim d^{-\beta}$, then the PZ plots are also influenced as can be observed in Fig. 6. The calculations in Fig. 6 were performed with $w=5(d/100)^{0.25}$, $\xi=100(d/100)^{2(0.25/H)}$, and $H=0.5$. With increasing metal thickness d the nonlinear behavior attenuates because in this particular case the local slope decreases ($\rho_{rms} \sim d^{-\beta}$) yielding thus surface smoothening. If the local slope increases logarithmically with film thickness $\rho_{rms} \sim \sqrt{\ln(d)}$, which is the case for anomalous self-affine growth (where due to insufficient surface diffusion of deposited metal atoms a groove instability develops leading to anomalous scaling) [23], the nonlinear behavior of the PZ plots will be further amplified with increasing deposited film thickness. At any rate, dynamic changes of the electrode roughness should be carefully quantified with respect to their influence on PZ plots and related systems.

IV. CONCLUSIONS

In this work, we have investigated the dependence of PZ plots on characteristic self-affine roughness parameters w, ξ, and H. It was shown that among all the characteristic roughness parameters, the roughness exponent H appears to have the most prominent effect. Moreover, with decreasing compact layer thickness the influence of roughness leads to stronger nonlinear behavior of the PZ plots for large electrode potentials ($e\beta\Phi_o \gg 1$). Finally, dynamic changes of the electrode roughness should be carefully quantified with respect to their influence on PZ plots and related studies where the presence of double layers is under consideration. Our examination indicates that the PZ plots can be sensitive to self-affine growth details when the local surface slope evolves with film thickness and/or the roughness exponent H does not remain constant.

ACKNOWLEDGMENTS

We would like to acknowledge support from the Nederlandse Organisatie voor Wetenschappelijk Onderzoek (NWO). We would also like to thank J. Th. M. DeHosson for useful comments.

[1] P. Delahay, *Double Layer and Electrode Kinetics* (Wiley, New York, 1966); E. Gileadi, E. Kirowa-Eisner, and J. Penciner, *Interfacial Electrochemistry* (Addison-Wesley, Reading, MA, 1975); B. B. Damaskin and O. A. Petrii, *Introduction to Electrochemical Kinetics* (Vyshaya Shkola, Moscow, 1975).

[2] J. N. Israelachvili, *Intermolecular and Surface Forces* (Academic, London, 1990).

[3] D. Andelman, in *Handbook of Physics of Biological Systems*, edited by R. Lipowsky (Elsevier, New York, 1994), p. 577.

[4] S. Liu, in *Condensed Matter Physics Aspects of Electrochemistry*, edited by M. P. Tosi and A. A. Kornyshev (World Scientific, Singapore, 1991), p. 329.

[5] G. Gouy, J. Phys. (Paris) **9**, 457 (1910); D. L. Chapman, Philos. Mag. **25**, 475 (1913).

[6] P. Debye and W. Huckel, Phys. Z. **24**, 185 (1924); **24**, 305 (1924); P. Debye, *ibid.* **25**, 97 (1924).

[7] A. N. Frumkin, *Potentials of Zero Charge* (Moscow, Nauka, 1979); R. Parsons, Usp. Khim. **21**, 681 (1976); B. B. Damaskin and R. V. Ivanova, Electrochim. Acta **48**, 1747 (1979); I. A. Bagotskaya and L. I. Shlepakov, Elektrokhimiya **16**, 565 (1980)

[8] M. A. Vorotyntsev, in *Modern Aspects of Electrochemistry*, edited by J. O'M. Bockris, B. E. Conway, and R. E. White (Plenum, New York, 1986), Vol. 17, p. 131.

[9] L. I. Daikhin, A. A. Kornyshev, and M. Urbakh, Phys. Rev. E **53**, 6192 (1996).

[10] E. Lust, A. Janes, V. Sammelselg, P. Miidla, and K. Lust, Electrochim. Acta **44**, 373 (1998).

[11] L. I. Daikhin, A. A. Kornyshev, and M. Urbakh, J. Chem. Phys. **108**, 1715 (1998).

[12] E. Lust, A. Janes, V. Sammelselg, and P. Miidla, Electrochim. Acta **46**, 185 (2000).

[13] A. Hamelin, M. L Foresti, and R. Guidelli, J. Electroanal. Chem. **346**, 251 (1993).

[14] M. L Foresti, R. Guidelli, and A. Hamelin, J. Electroanal. Chem. **346**, 73 (1993).

[15] A. Bagotskaya, B. B. Damaskin, and M. D. Levi, J. Electroanal. Chem. Interfacial Electrochem. **115**, 189 (1980).
[16] G. Valete, J. Electroanal. Chem. Interfacial Electrochem. **260**, 425 (1989).
[17] A. A. Kornyshev, W. Schmickler, and M. A. Vorotyntsev, Phys. Rev. B **25**, 5244 (1982).
[18] B. N. J. Persson and E. Tosatti, J. Chem. Phys. **115**, 3840 (2001).
[19] G. Palasantzas and G. M. E. A. Backx, Surf. Sci. **540**, 401 (2003); G. Palasantzas and G. Backx, J. Chem. Phys. **118**, 4631 (2003).
[20] P. Meakin, Phys. Rep. **235**, 1991 (1994); J. Krim and G. Palasantzas, Int. J. Mod. Phys. B **9**, 599 (1995); F. Family and T. Viscek, *Dynamics of Fractal Surfaces* (World Scientific, Singapore, 1991).
[21] G. Palasantzas, Phys. Rev. B **48**, 14 472 (1993); **49**, 5785(E) (1994).
[22] G. Palasantzas, Phys. Rev. E **56**, 1254 (1997).
[23] J. H. Jeffries, J.-K. Zuo, and M. M. Craig, Phys. Rev. Lett. **76**, 4931 (1996).